ARTICLES
https://doi.org/10.1038/s41929-020-00569-8

nature catalysis

Check for updates

Gold-catalysed asymmetric net addition of unactivated propargylic C–H bonds to tethered aldehydes

Ting Li[1,2,3,4], Xinpeng Cheng[1,4], Pengcheng Qian[2]✉ and Liming Zhang[1]✉

The asymmetric one-step net addition of unactivated propargylic C–H bonds to aldehydes leads to an atom-economic construction of versatile chiral homopropargylic alcohols, but has not yet been realized. Here we show its implementation in an intramolecular manner under mild reaction conditions. This chemistry—via cooperative gold catalysis enabled by a chiral bifunctional phosphine ligand—achieves asymmetric catalytic deprotonation of propargylic C–H ($pK_a > 30$) by a tertiary amine group ($pK_a \approx 10$) of the ligand in the presence of much more acidic aldehydic α-hydrogens ($pK_a \approx 17$). The reaction exhibits a broad scope and readily accommodates various functional groups. The cyclopentane/cyclohexane-fused homopropargylic alcohol products are formed with excellent enantiomeric excesses and high *trans*-selectivities with or without a preexisting substrate chiral centre. Density functional theory studies of the reaction support the conceived reaction mechanism and the calculated energetics corroborate the observed stereoselectivity and confirm additional metal–ligand cooperation.

Asymmetric propargylation of aldehydes leads to versatile chiral homopropargylic alcohol products and is of exceptional importance in organic synthesis[1,2]. To achieve asymmetry in these reactions, allenylmetal species featuring Si, B, Al, Cu, Sn, Cr, In (and so on) serve as the propargylic nucleophile and are either prepared beforehand or generated in situ via transmetallation with a propargylmetal precursor, or from propargylic halides in the presence of reducing metal (Fig. 1a). This requirement of prefunctionalization at the propargylic position is conceptually much less appealing than the direct asymmetric net addition of a propargylic C–H bond to a carbonyl group as the latter process is completely atom economic, avoids the use of stoichiometric metal and/or costly substrates and the generation of stoichiometric metal salt waste, and could be achieved via sequential deprotonation–propargylation–protonation in a catalytic manifold. This type of chemistry constitutes a catalytic asymmetric propargylic C–H functionalization[3–11] but to the best of our knowledge remains undocumented in literature. In the recently reported racemic case[11], aldehyde substrates possessing α-C(sp^3)–H bonds are not permitted. Such substrates are challenging and seem to not be conceptually feasible under typical basic conditions as the propargylic protons are much less acidic ($pK_a > 30$) than aldehyde α-hydrogens ($pK_a \approx 17$) in an ionic reaction manifold (Fig. 1b). Self-aldol reaction/condensation would instead be the dominant reaction pathway.

In an earlier report by our laboratory[12], we realized net addition of a propargylic C–H bond to an aldehyde in a propargylation reaction under homogeneous Au(I) catalysis. As shown in Fig. 1c, in the presence of a gold(I) catalyst that contains the achiral biphenyl-2-ylphosphine ligand **L1** (which features a remote tertiary amino group[13–17]), the intermolecular propargylation of an aldehyde by a silylated alkyne occurs smoothly and the generated homopropargylic alcohol **1** undergoes further silyl-migrative cyclization to deliver the dihydrofuran product **2** (ref. [18]); mechanistic studies confirmed the intermediacy of **1**. The reaction is proposed to proceed via a σ-allenylgold intermediate (that is, **A**), the generation of which entails the deprotonation of the propargylic C–H bond ($pK_a > 30$) by the ligand tertiary amino group ($pK_a \approx 10$), which is enabled by the cooperative activation of C≡C by the appropriately positioned Lewis acidic gold(I) centre. Aside from being racemic, this reaction suffers limitations in scope: the propargylic C–H bond needs to be activated by an aryl/alkenyl substituent and the aldehyde needs to be activated by an electron-deficient unsaturated group and cannot accommodate any α-C(sp^3)–H bonds.

In this work we report the asymmetric intramolecular net addition of an unactivated propargylic C–H bond to aldehydes in a catalytic manner. By developing a chiral bifunctional ligand, the reactions exhibit mostly excellent enantioselectivities and diastereoselectivities, and tolerate aldehydes that possess α-C(sp^3)–H bonds. The chemoselective deprotonation, ready accommodation of a preexisting substrate chiral centre of either configuration, and the high synthetic value of the cyclic products, are of great significance.

Results

Reaction discovery and optimization. At the outset, we chose the *tert*-butyldimethylsilyl (TBS)-terminated hept-6-ynal (**3a**) as the substrate for reaction discovery and optimization. It was anticipated that chemoselective deprotonation of its propargylic H_a over the aldehydic H_b—despite the latter being more acidic—in the presence of cationic gold(I), ligated by our recently developed bifunctional phosphine ligand, was plausible due to the above-discussed cooperative deprotonation of propargylic C–H bonds by the mildly basic ligand tertiary amine. Such a process would generate a nucleophilic σ-allenylgold intermediate and hence permit cyclization to form the *trans*-ring-fused homopropargylic alcohol **4a** and its *cis*-isomer in a catalytic setting. With achiral **L1** as the ligand and the reaction temperature at 60 °C, **4a** was indeed formed as the major product along

[1]Department of Chemistry and Biochemistry, University of California, Santa Barbara, CA, USA. [2]Key Laboratory of Environmental Functional Materials Technology and Application of Wenzhou City, College of Chemistry & Materials Engineering, Institute of New Materials & Industry Technology, Wenzhou University, Wenzhou, China. [3]Present address: College of Chemistry and Pharmaceutical Engineering, Nanyang Normal University, Nanyang, Henan, P. R. China. [4]These authors contributed equally: Ting Li, Xinpeng Cheng. ✉e-mail: qpc@wzu.edu.cn; zhang@chem.ucsb.edu

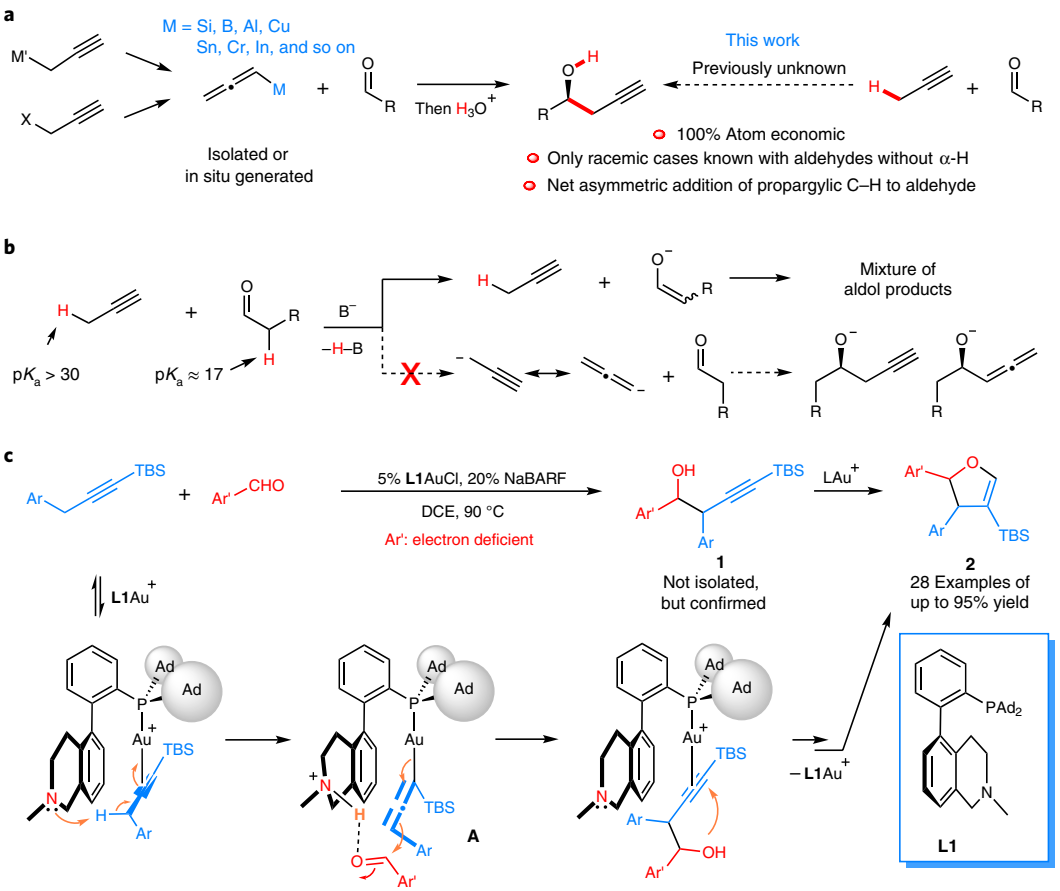

Fig. 1 | Asymmetric propargylation of aldehydes. a, Strategies for asymmetric propargylation of aldehydes. **b**, The challenges involved in directly reacting propargylic C–H bonds with aldehydes that possess α-hydrogens. **c**, Our previous work: intermolecular net racemic addition of a propargylic C–H bond to an aldehyde without α-C–H bond.

with **4a**′, **4a**″ and **4a**‴ (entry 1). It should be noted that the *cis*-**4a** was not detected from the reaction mixture. It seems that **4a**′, **4a**″ and **4a**‴ were generated from *cis*-**4a** as the *trans* product **4a** could not be converted to these side products under identical reaction conditions. Unsurprisingly, JohnPhos—a biphenylphosphine ligand similar to **L1** with regards to electronics and sterics but lacking the remote amino group—led to no reaction at all, and the addition of Et_3N did not help either (entries 2 and 3). These results again highlight the cooperating role of the ligand amino group in the gold catalysis.

With this encouraging result in hand, we turned our attention to asymmetric catalysis. We previously developed the ligand (*R*)-**L2** (a chiral version of **L1**) for the asymmetric isomerization of alkynes to chiral allenes en route to chiral dihydrofuran products[19]. The general design considerations leading to the chiral ligand are shown in Table 1, that is, the R group at the ligand chiral centre can shield the basic nitrogen from participating in the reaction in one of the two biaryl axis configurations, and consequently the ligand centre chirality can be employed to achieve the desired ligand axis chirality for asymmetric gold catalysis. Coupled with the fluxional nature of the axis, both atropisomers of the catalyst may effectively participate in catalysis. In that reaction, a chiral *σ*-allenylgold intermediate of type **A** (see Fig. 1c) is generated en route to a chiral allene intermediate. It was reasoned that with (*R*)-**L2** as the ligand this intramolecular propargylation could become enantioselective. Much to our delight, with (*R*)-**L2**Au$^+$ as the catalyst, the cyclization delivered **4a** in 55% yield in −93% e.e. (its configurations are opposite to those in the shown structure, entry 4).

We further optimized the ligand to improve this reaction. Our density functional theory (DFT) calculations of the tetrahydroisoquinoline portion of **L2** at the M06-2X/cc-pVDZ level revealed that the nitrogen-exposed conformer **B** is 3.61 kcal mol^{-1} less stable than the nitrogen-buried conformer **B**' due to the gauche interaction between *N*-Me and the cyclohexyl group in **B**; the desired **B** is therefore a minor conformer. We reasoned that minimizing the cyclohexyl group into a methyl group would decrease the destabilizing gauche interaction and make **B** energetically less disfavoured. To maintain pseudo-axial orientation of the 1-methyl group, a 8-methyl group should be installed to enhance $A^{1,3}$-strain when it is pseudo-equatorially oriented. DFT calculations indeed confirmed that the two conformations of 1,8,*N*-trimethyltetrahydroquinoline (**C** and **C**') are energetically nearly equal. To this end, the corresponding ligand (*S*)-**L3** was prepared and its structure was confirmed by X-ray diffraction studies of its AuCl complex (Fig. 2a; see Supplementary Section "Synthesis of Ligands and Catalysts" for details). It led to a better yield of **4a** (77%) and an excellent e.e. (99%, entry 5). Compounds **4a**', **4a**″ and **4a**‴ were barely detected, indicating a *trans*/*cis* selectivity of >13 in the cyclization step. The absolute configuration of **4a** was assigned based on the X-ray diffraction study of one of its homologues (Fig. 2b). The counter anion of the in situ-generated cationic gold(I) catalyst is also of critical importance, and only tetrakis[3,5-bis(trifluoromethyl)-phenyl]borate ([BARF$^-$]) worked well. The use of other commonly employed anions such as OTf$^-$ (entry 6) and NTf_2^- (entry 7) resulted in no products at all. The reaction yield was 40% when $Ag(CH_3CN)_2^+$ BARF$^-$ was used instead of NaBARF (entry 8). Furthermore, the

Table 1 | Reaction discovery and condition optimization

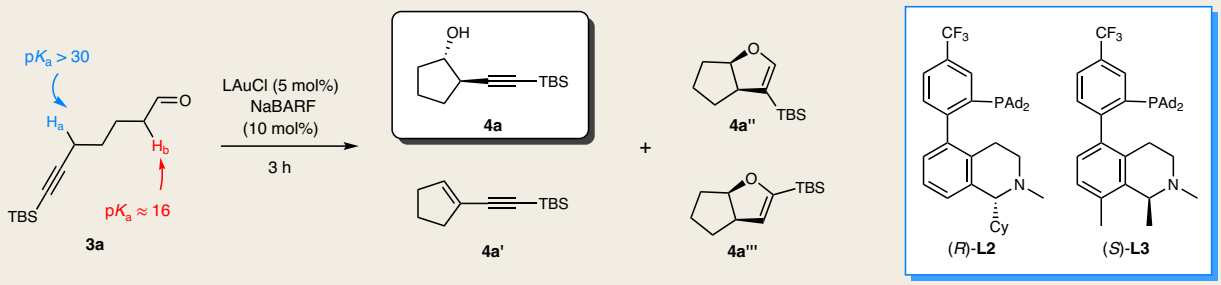

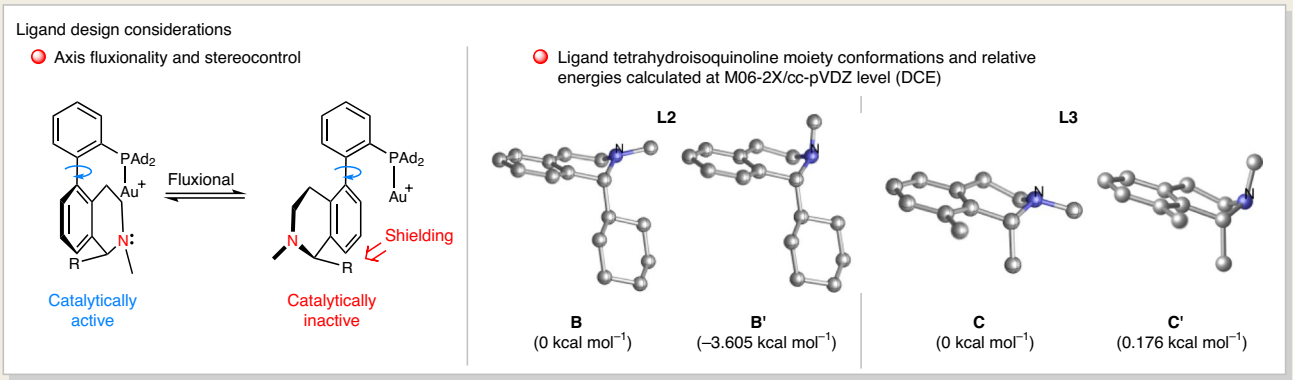

Entry	Ligand	Reaction conditions (3h)	Conversion (%)	Yield (%)[a] 4a/4a'/4a''/4a'''	e.e. (%)[b] (4a)
1	**L1**	NaBARF (10 mol%), DCE, 60 °C	95	49/8/8/15	—
2	JohnPhos	NaBARF (10 mol%), DCE, 60 °C	0	0	—
3	JohnPhos	NaBARF (10 mol%), DCE, 60 °C, 10% Et_3N	0	0	—
4	(*R*)-**L2**	NaBARF (10 mol%), DCE, r.t.	70	55/—/—/—	–93
5	(*S*)-**L3**	NaBARF (10 mol%), DCE, r.t.	95	77/0/<3/<3	99
6	(*S*)-**L3**	AgOTf (10 mol%), DCE, r.t.	<10	0	—
7	(*S*)-**L3**	$AgNTf_2$ (10 mol%), DCE, r.t.	<10	0	—
8	(*S*)-**L3**	$Ag(CH_3CN)_2BARF$ (10 mol%), DCE, r.t.	60	40/—/—/—	99
9	(*S*)-**L3**	NaBARF (10 mol%), $PhCF_3$, r.t.	60	32/—/—/—	99
10	(*S*)-**L3**	NaBARF (10 mol%), THF, r.t.	57	33/—/—/—	99

All reactions were run in sealed vials without replacing the atmosphere with argon or N_2. [a]Isolated yields. [b]Determined by HPLC using a corresponding benzyl ester. DCE, 1,2-dichloroethane; THF, tetrahydrofuran; NaBARF, sodium tetrakis[3,5-bis(trifluoromethyl)phenyl]borate; JohnPhos, (2-biphenyl)di-*tert*-butylphosphine.

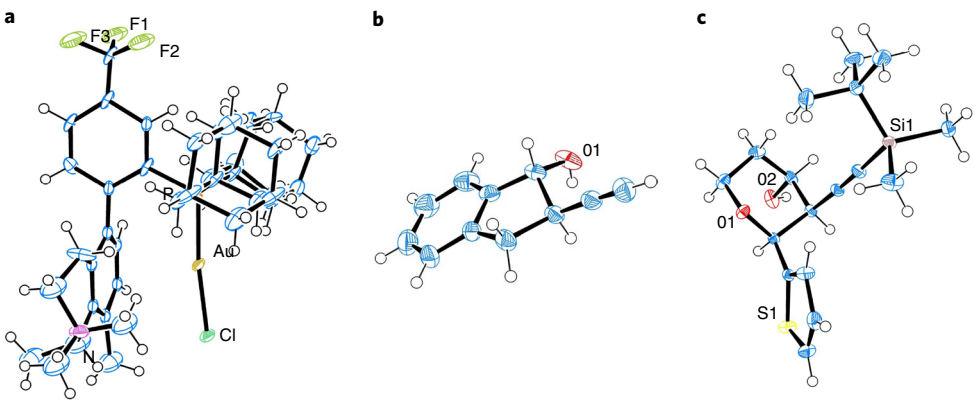

Fig. 2 | Oak Ridge thermal ellipsoid plots of crystal structures. a, The X-ray structure of (*S*)-**L3**AuCl (crystal CH_2Cl_2 has been omitted; both *N*-methyl conformers were detected). **b**, The X-ray structure of **11**. **c**, The X-ray structure of (2*S*,3*R*,4*S*)-**6p**. Ellipsoid probability was at 50%. Green, fluorine; grey, carbon; orange, phosphorus; gold, gold; tan, silicon; blue, nitrogen; red, oxygen; white, hydrogen.

Table 2 | Scope toward the formation of five-membered ring-fused homopropargylic alcohols[a]

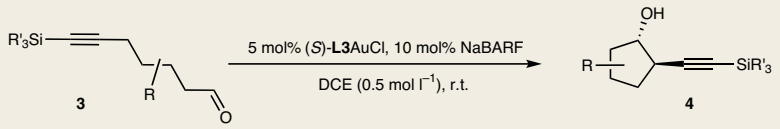

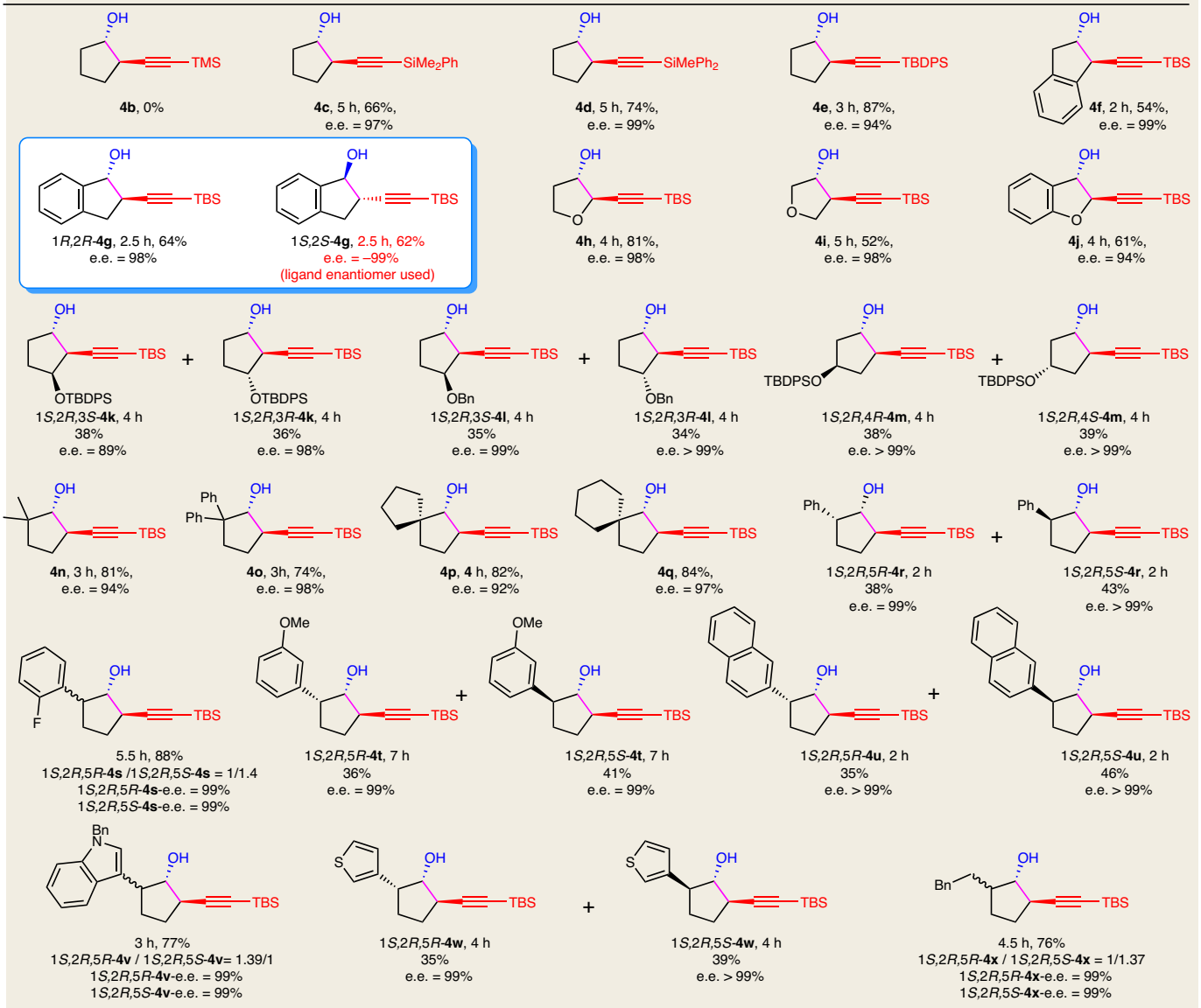

[a]All reactions were run in sealed vials with an initial substrate concentration of 0.5 M.

solvent DCE is important for the optimal yield as $PhCF_3$ and THF led to lower yields (entries 9 and 10).

Reaction scope studies. With the optimized reaction conditions in hand, we set out to investigate the reaction scope. First, silyl-protecting groups other than TBS were examined. As shown in Table 2, the much smaller TMS group led to no target product **4b**, and only the aldehyde oxidation product 7-(trimethylsilyl) hept-6-ynoic acid was detected. Furthermore, running the reaction under argon did not permit the desired reaction, either. However, other bulkier silyl groups including $SiMe_2Ph$ (**4c**), $SiMePh_2$ (**4d**) and TBDPS (**4e**) were allowed, and TBDPS led to an excellent yield but a slightly lower e.e. value. Further studies revealed that instalment of a fused benzene ring into the substrate backbone was allowed, and products **4f** and **4g** were obtained in moderate yields and with excellent enantioselectivities. Switching the chiral ligand to its enantiomer led to essentially identical results with the opposite product stereochemistry. Substrates containing oxygen at different positions of the backbone all underwent the reaction smoothly, affording the tetrahydrofuran or dihydrofuran products **4h**, **4i** and **4j** with excellent e.e. value. Dihydrobenzofuranol 11—prepared following desilylation of **4j**—was subjected to X-ray diffraction studies. As shown in Fig. 2b, it exhibits the (1*R*, 2*R*)-configuration. Consequently, the configurations of the nascent chiral centres of all of the five-membered ring products were assigned accordingly. Substituents of varying electronic and steric characteristics were generally allowed in this transformation, leading to products **4k**–**4x** in good yields and excellent enantioselectivities. It should be noted that some of the products (**4k**–**4m** and **4r**–**4x**) possess an extra stereocentre and were synthesized from the corresponding racemic

Table 3 | Reaction optimization for the formation of six-membered-ring-fused homopropargylic alcohols

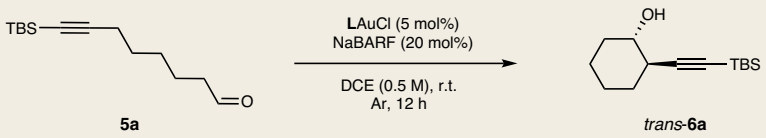

5a trans-6a

Entry	Ligand	Conversion	Yield (%)[a]	e.e. (%)[b]
1[c]	(*S*)-**L3**	<10	0	-
2	(*S*)-**L3**	95	70	98
3	(*R*)-**L2**	95	65	−76
4	(*R*)-**L3**	95	70	−99

All reactions were run in sealed vials. [a]Isolated yields. [b]Determined by HPLC using a corresponding benzyl ester. [c]The reaction was run under air and 10 mol% NaBARF was used.

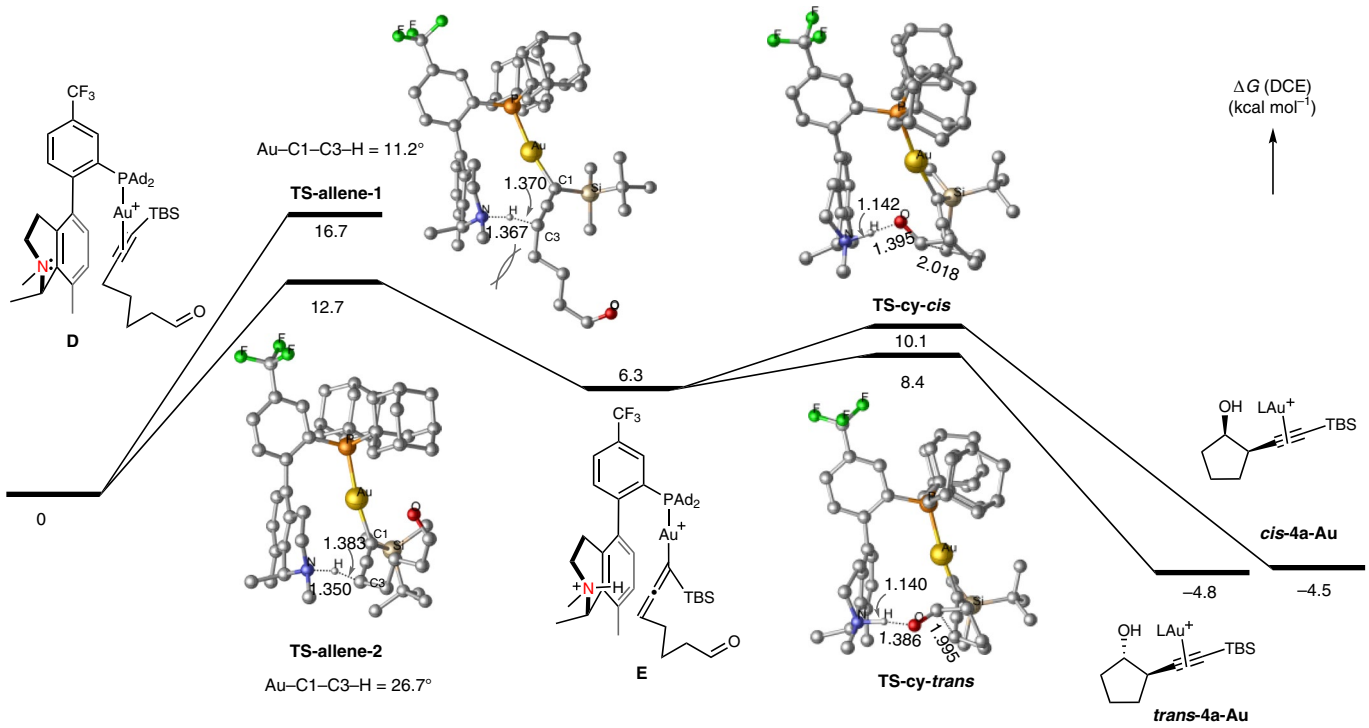

Fig. 3 | DFT-calculated energetics of the reaction of 3a in DCE. DFT calculations were performed at the PBE1PBE level using the effective core potential LANL2DZ for gold, basis set 6-311g(*d*,*p*) for silicon and phosphorus, and 6-31g(*d*,*p*) for the other atoms. The solvent model based on density (SMD) is employed for solvent DCE. The numbers by the energy levels are the Δ*G* values in DCE solvent, given in kcal mol^{-1}. The bond distances overlaying the structures are in angstroms.

substrates. The exceptional levels of asymmetric induction (mostly ≥98% e.e.) with either substrate enantiomer highlight the extraordinary catalyst-dictated asymmetric induction independent of substrate chirality, a highly valuable feature in asymmetric catalysis that permits flexible and selective access to different product stereoisomers by simply varying substrate and catalyst chirality. Some of the diastereomeric products (**4k**–**m**, **4r**, **4t**, **4u** and **4w**) are separable and were individually characterized. In all cases, with the exception of **4m**, the configurations of the stereogenic centres inherited from substrates were assigned based on the splitting pattern of the middle carbon proton of the stereochemical triad, where a triplet with $^3J_{H-H}$ ranging from 5 to 9 Hz in one stereoisomer is assigned to the *trans*–*trans* arrangement, whereas its epimer displays a doublet of doublets or a pseudo triplet with $^3J_{H-H}$ at around 2–3 Hz and hence is assigned to the *trans*–*cis* arrangement. These assignments are further supported in some cases by the observed nuclear overhauser effect as well as related literature observations[20–22]. The stereochemistry of **4m** was tentatively assigned by assuming that the alkynyl group of the 1*S*, 2*R*, 4*S*-isomer is in the bisected position and that the HO and TBDPSO (*tert*-butyldiphenylsiloxy) groups are in equatorial positions in an envelope conformer. Notably, the substrates bearing severe steric hindrance all worked well in this chemistry, resulting in the formation of **4n**–**4q** in good yields and indicating that the steric hindrance around the aldehyde group is inconsequential. Replacing the phenyl group of **4r** with other aryl groups, including 2-naphthyl (**4u**), 3-indolyl (**4v**) and 3-thienyl (**4w**), was also successful. We also examined the alkyl group in place of the **4r** phenyl group, and the desired product **4x** was smoothly formed.

It is worth noting that we could not find asymmetric chemical synthesis of desilylated **4a** (the simplest structure in the reaction scope) in the literature despite its commercial availability. The stereochemically more complex **4k**–**4m** and **4r**–**4x** present further

Table 4 | The scope towards the formation of six-membered-ring-fused homopropargylic alcohols

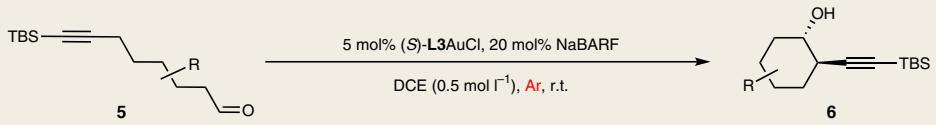

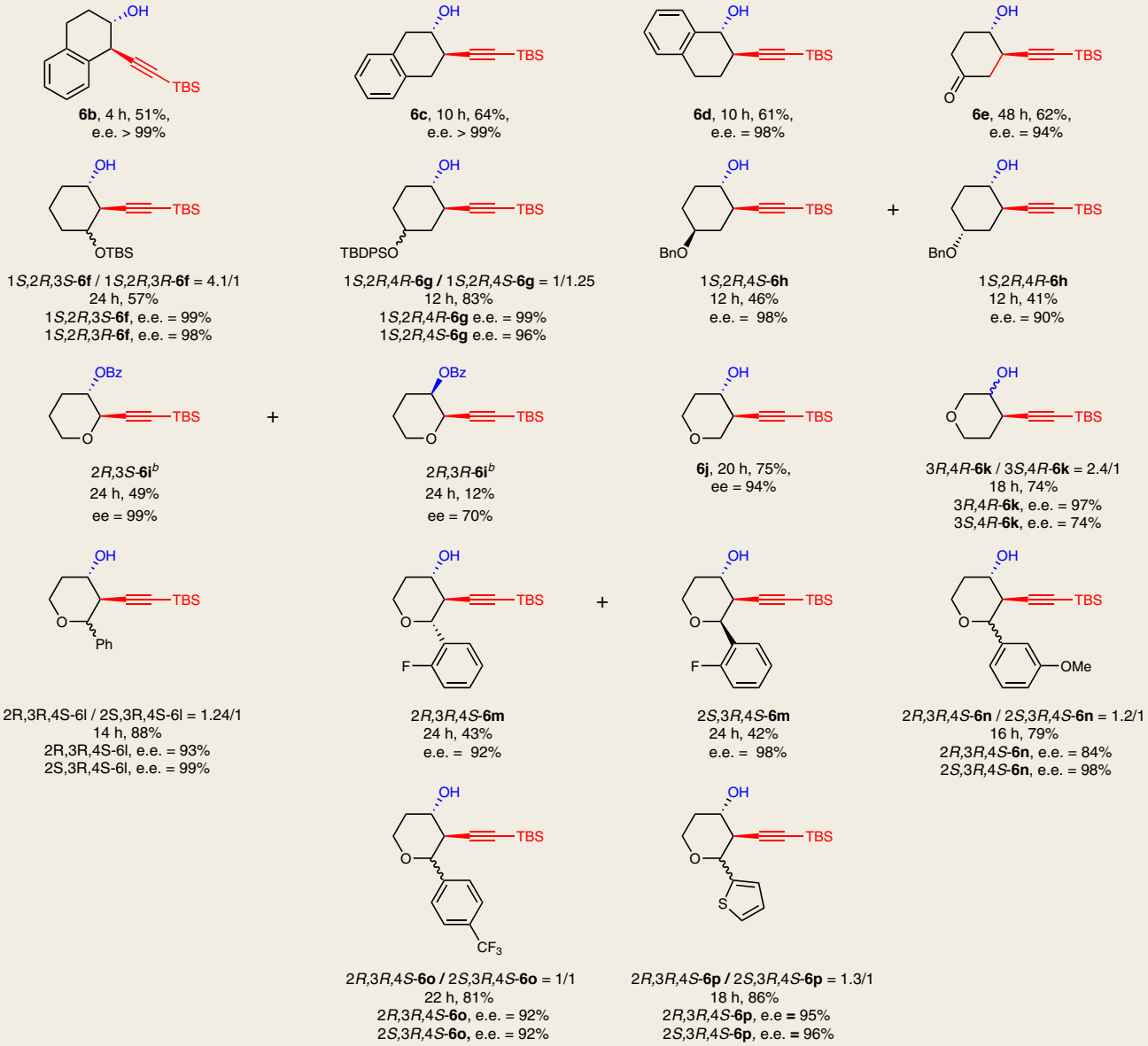

All reactions were run in sealed vials with an initial substrate concentration of 0.5 M. [a]The products were converted to benzoates and then separated.

synthetic challenges, especially considering the issues associated with regioselectivity in the synthetic approach employing epoxide ring opening (for example, **4k** and **4l**; ref. [23]) and the inevitable shortcomings of stereochemical inflexibility due to substrate stereocontrol. This chemistry, on the other hand, provides a general, highly stereoselective and stereoflexible strategy to access these synthetically valuable cyclopentanols.

We then turned our attention to the asymmetric construction of six-membered-ring-fused homopropargylic alcohols. The brief reaction optimization is shown in Table 3. Initially, no desired product **6a** was formed under the conditions optimized for the cyclopentanol formation (entry 1); however, it was later found that the reaction of **5a** delivered the desired product *cis*-**6a** in 70% yield and with 98% e.e when the reaction was performed under argon and with 20 mol% NaBARF (entry 2). The opposite high enantioselectivity was realized with (*R*)-**L3** as the ligand (entry 4). However, (*R*)-**L2** is a markedly inferior ligand for the asymmetric induction, resulting in only −76% e.e. (entry 3).

The reaction scope was then investigated. As shown in Table 4, benzene fusions at the substrate backbone were allowed, and the anticipated *trans*-homopropargylic alcohol products **6b**, **6c** and **6d** were obtained in serviceable yields and with excellent enantioselectivities. Oxygen-based substituents, whether an oxo (**6e**), siloxyl (**6f** or **6g**) or BnO (**6h**), were tolerated and the reactions again exhibited excellent asymmetric induction, regardless of the preexisting stereochemistry in the case of **6f**–**6h**. In the case of **6f**,

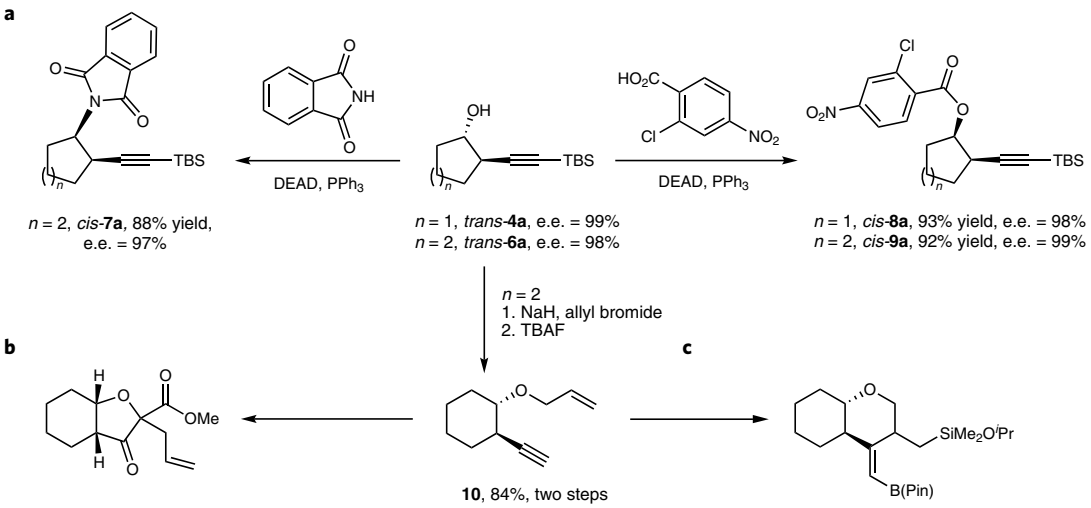

Fig. 4 | Further transformations of the products. a, Mitsunobu reactions. DEAD, diethyl azodicarboxylate. **b**, A reported oxidative rearrangement[25]. **c**, A reported silaborative cyclization[26].

the relatively high ratio of the diastereomeric products reveals that the substrate (*S*)-enantiomer exhibits substantially higher reactivity than its (*R*)-enantiomer. This is unusual as in most cases substrate enantiomers exhibit similar reactivities. Substrates containing oxygen in the linker between the reacting functional groups were also tested, and the *trans*-tetrahydropyran products **6i**, **6j** and **6k** were formed with excellent enantioselectivities. In the cases of **6i** and **6k**, the corresponding *cis*-isomers were also detected as the minor product and interestingly with markedly lower e.e. Of note, **6i** was characterized as separable benzoates. A phenyl substitution at the homopropargylic position of **6j** in the case of **6l** was readily permitted, and the substrate chirality again had little impact on the ligand-imposed asymmetric induction, affording both epimers of the trisubstituted tetrahydropyran **6l** in a combined yield of 88% and with excellent e.e. Moreover, different substitutions on the phenyl ring—including *ortho*-F (**6m**), *meta*-MeO (**6n**) and *para*-CF_3 (**6o**) or its replacement with a 2-thiophenyl (**6p**)—were readily accommodated, and the tetrahydropyran products were isolated in good yields and with e.e. values ranging from 92% to 98%. Although **6p** was isolated as a chromatographically inseparable viscous liquid at room temperature, one isomer crystallized out following storage at −20 °C in a freezer and its X-ray diffraction studies established the configurations of its newly generated stereocentres as 3*R*, 4*S*, which are identical to those in the five-membered ring products (Fig. 2c). Consequently, the configurations of these nascent stereocentres in the other products **6** were assigned accordingly. The configurations of the inherited chiral centres in **6f**–**6h** and **6l**–**6o** were assigned based on ^{1}H–^{1}H coupling patterns.

To the best of our knowledge, there is no reported synthetic method for the desilylated (1*S*, 2*R*)-**6a** nor general highly stereoselective access to the six-membered-ring-fused homoproparyglic alcohols shown in Table 4. Considering the ubiquity of these ring systems, this chemistry would prove to be of significant synthetic value.

DFT calculations. We performed DFT studies of the reaction of **3a** to gain insights into the reaction mechanism and to understand the observed stereoselectivities. As shown in Fig. 3, the deprotonation transition state **TS-allene-2** leading to the allenylgold intermediate **E** with an (*aR*)-allene is favoured by 4.0 kcal mol^{-1} over **TS-allene-1**. This difference in activation energy can be largely attributed to the indicated steric congestion in the latter and consistent with the observed high enantioselectivities. The deprotonation follows a *syn*-periplanar process[24] with the dihedral angle of Au-C1–C3-H being 11.2° in **TS-allene-1** and 26.7° in **TS-allene-2**. Subsequent cyclizations of the kinetically favoured allenylgold **E** only need to overcome a barrier of 3.8 kcal mol^{-1} or 2.1 kcal mol^{-1} to form the gold-coordinated cyclopentanols ***cis*-4a-Au** or ***trans*-4a-Au**, respectively. These barriers are much lower than the 6.4 kcal mol^{-1} needed for **E** to revert back to **D**, suggesting that the equilibrium between **E** and its allene epimer via **D** is not operative. The *trans*-cyclization leading to ***trans*-4a-Au** is favoured by 1.7 kcal mol^{-1} with regard to the reaction barrier over the competing *cis*-cyclization, despite little difference in product stability. This is consistent with the observed formation of **4a** as the major product. Moreover, the distances between the ligand ammonium proton and the aldehyde oxygen are 1.395 Å and 1.386 Å in **TS-cy-cis** and **TS-cy-trans**, respectively, indicating activation of the aldehyde by the acidic ligand proton and confirming additional cooperation between metal and ligand in the chemistry. Finally, the configurations of the cyclopentanol moiety in ***trans*-4a-Au** are identical to our experimental assignments.

Synthetic applications. The presence of a hydroxyl group in the products provided a versatile handle for further functionalization. As shown in Fig. 4a, the products *trans*-**4a** or *trans*-**6a** could be easily transformed to *cis*-**7a**, *cis*-**8a** and *cis*-**9a** in excellent yields and enantiopurities via the Mitsunobu reaction. These results established that all four stereoisomers of the fused homopropargylic alcohols can be accessed with high to excellent stereoselectivity via this gold catalysis, which is of considerable synthetic value. The products could also be easily transformed into the 1,7-enynes derivative **10**, which can undergo cyclization/cycloisomerization to afford the bicyclic dihydrofuran-3-one in Fig. 4b (ref. [25]) and the silaborative carbocyclization product in Fig 4c (ref. [26]) by following the literature procedures.

Conclusions

We have achieved catalytic asymmetric net addition of an unactivated propargylic C–H bond to a tethered aldehyde. Employing a ligand-enabled cooperative gold catalysis, this reaction realizes selective deprotonation of propargylic C–H ($pK_a > 30$) by a rather weak tertiary amino group ($pK_a \approx 10$) in the presence of substantially more acidic aldehydic α-hydrogens ($pK_a \approx 17$). Aldehydes that possess α-C(sp^3)–H (which were not permitted in two precedents) are readily tolerated by this reaction, and the five/six-membered-ring-fused products are generated with excellent enantiomeric excesses and diastereoselectivities. For substrates possessing a chiral centre in either

configuration, this asymmetric gold catalysis maintains exceptional levels of asymmetric induction, affording ring-fused homopropargylic alcohol products with increasing stereochemical complexity. These chiral cyclopentanols and cyclohexanols should be of exceptional synthetic values, yet the preparation of these products is synthetically challenging. This chemistry provides a facile access to them. DFT studies support the conceived mechanism, corroborate the stereochemical assignments and the observed stereoselectivity, and confirm ligand–metal cooperation in the cyclization step. This propargylic C–H functionalization strategy opens a highly valuable venue to further asymmetrically transform unactivated alkynes α-C–H bonds under mild catalytic conditions.

Methods

General synthetic procedure for chiral homopropargylic alcohol 4. A 3-dram vial with a magnetic stir bar was charged with aldehyde **3** (0.2 mmol), NaBARF (0.02 mmol, 17.7 mg, 10 mol%), **L3**AuCl (0.01 mmol, 8.5 mg, 5 mol%) and dry DCE (0.4 ml). The vial was sealed with a cap and stirred at room temperature. Reaction progress was monitored by thin-layer chromatography. Upon completion, the reaction was concentrated under reduced pressure. The residue was purified by silica gel flash column chromatography to obtain the desired product.

Data availability

Experimental procedures, characterization of compounds and DFT calculations are available in the Supplementary Information. The X-ray diffraction data for **11**, **6p** and (*S*)-**L3**AuCl are deposited to the Cambridge Crystallographic Data Centre (CCDC) with the reference numbers 1988012, 1988013 and 1988482, respectively. All data are available from the authors on reasonable request.

Received: 21 March 2020; Accepted: 15 December 2020;
Published online: 18 February 2021

References

1. Ding, C.-H. & Hou, X.-L. Catalytic asymmetric propargylation. *Chem. Rev.* **111**, 1914–1937 (2011).
2. Yang, X., Kalita, S. J., Maheshuni, S. & Huang, Y.-Y. Recent advances on transition-metal-catalyzed asymmetric tandem reactions with organoboron reagents. *Coord. Chem. Rev.* **392**, 35–48 (2019).
3. Alvarez, L. X., Christ, M. L. & Sorokin, A. B. Selective oxidation of alkenes and alkynes catalyzed by copper complexes. *Appl. Catal. A* **325**, 303–308 (2007).
4. Cheng, D. & Bao, W. Propargylation of 1,3-dicarbonyl compounds with 1,3-diarylpropynes via oxidative cross-coupling between sp^3 C–H and sp^3 C–H. *J. Org. Chem.* **73**, 6881–6883 (2008).
5. Grigg, R. D., Rigoli, J. W., Pearce, S. D. & Schomaker, J. M. Synthesis of propargylic and allenic carbamates via the C–H amination of alkynes. *Org. Lett.* **14**, 280–283 (2012).
6. Wang, T., Zhou, W., Yin, H., Ma, J.-A. & Jiao, N. Iron-facilitated oxidative dehydrogenative C–O bond formation by propargylic C–H functionalization. *Angew. Chem. Int. Ed.* **51**, 10823–10826 (2012).
7. Lu, H., Li, C., Jiang, H., Lizardi, C. L. & Zhang, X. P. Chemoselective amination of propargylic C(sp^3)–H bonds by cobalt(II)-based metalloradical catalysis. *Angew. Chem. Int. Ed.* **53**, 7028–7032 (2014).
8. Fernández-Salas, J. A., Eberhart, A. J. & Procter, D. J. Metal-free CH–CH-type cross-coupling of arenes and alkynes directed by a multifunctional sulfoxide group. *J. Am. Chem. Soc.* **138**, 790–793 (2016).
9. Hu, G., Xu, J. & Li, P. Sulfur mediated propargylic C–H alkylation of alkynes. *Org. Chem. Front.* **5**, 2167–2170 (2018).
10. Ju, M. et al. Silver-catalyzed enantioselective propargylic C–H bond amination through rational ligand design. *J. Am. Chem. Soc.* **142**, 12930–12936 (2020).
11. Wang, Y., Zhu, J., Durham, A. C., Lindberg, H. & Wang, Y.-M. α-C–H Functionalization of π-bonds using iron complexes: catalytic hydroxyalkylation of alkynes and alkenes. *J. Am. Chem. Soc.* **141**, 19594–19599 (2019).
12. Li, T. & Zhang, L. Bifunctional biphenyl-2-ylphosphine ligand enables tandem gold-catalyzed propargylation of aldehyde and unexpected cycloisomerization. *J. Am. Chem. Soc.* **140**, 17439–17443 (2018).
13. Wang, Z., Wang, Y. & Zhang, L. Soft propargylic deprotonation: designed ligand enables Au-catalyzed isomerization of alkynes to 1,3-dienes. *J. Am. Chem. Soc.* **136**, 8887–8890 (2014).
14. Wang, Z., Ying, A., Fan, Z., Hervieu, C. & Zhang, L. Tertiary amino group in cationic gold catalyst: tethered frustrated lewis pairs that enable ligand-controlled regiodivergent and stereoselective isomerizations of propargylic esters. *ACS Catal.* **7**, 3676–3680 (2017).
15. Li, X., Ma, X., Wang, Z., Liu, P.-N. & Zhang, L. Bifunctional phosphine ligand enabled gold-catalyzed alkynamide cycloisomerization: access to electron-rich 2-aminofurans and their Diels–Alder adducts. *Angew. Chem. Int. Ed.* **58**, 17180–17184 (2019).
16. Li, X., Wang, Z., Ma, X., Liu, P.-N. & Zhang, L. Designed bifunctional phosphine ligand-enabled gold-catalyzed isomerizations of ynamides and allenamides: stereoselective and regioselective formation of 1-amido-1,3-dienes. *Org. Lett.* **19**, 5744–5747 (2017).
17. Wang, H., Li, T., Zheng, Z. & Zhang, L. Efficient synthesis of α-allylbutenolides from allyl ynoates via tandem ligand-enabled Au(I) catalysis and the Claisen rearrangement. *ACS Catal.* **9**, 10339–10342 (2019).
18. Li, T., Yang, Y., Li, B., Bao, X. & Zhang, L. Gold-catalyzed silyl-migrative cyclization of homopropargylic alcohols enabled by bifunctional biphenyl-2-ylphosphine and DFT studies. *Org. Lett.* **21**, 7791–7794 (2019).
19. Cheng, X., Wang, Z., Quintanilla, C. D. & Zhang, L. Chiral bifunctional phosphine ligand enabling gold-catalyzed asymmetric isomerization of alkyne to allene and asymmetric synthesis of 2,5-dihydrofuran. *J. Am. Chem. Soc.* **141**, 3787–3791 (2019).
20. Schnabel, C. et al. Total synthesis of natural and non-natural $\Delta^{5,6}\Delta^{12,13}$-jatrophane diterpenes and their evaluation as MDR modulators. *J. Org. Chem.* **76**, 512–522 (2011).
21. Dahlmann, H. A., McKinney, A. J., Santos, M. P. & Davis, L. O. Organocatalyzed intramolecular carbonyl–ene reactions. *Molecules* **21**, 713 (2016).
22. Amarasinghe, K. K. D. & Montgomery, J. Enantioselective total synthesis of (+)-testudinariol a using a new nickel-catalyzed allenyl aldehyde cyclization. *J. Am. Chem. Soc.* **124**, 9366–9367 (2002).
23. Zhou, J., Yang, M., Akdag, A. & Schneller, S. W. C-4′ Truncated carbocyclic formycin derivatives. *Tetrahedron* **62**, 7009–7013 (2006).
24. Basak, A., Chakrabarty, K., Ghosh, A. & Das, G. K. Theoretical study on the isomerization of propargyl derivative to conjugated diene under Au(I)-catalyzed reaction: a DFT study. *Comput. Theor. Chem.* **1083**, 38–45 (2016).
25. Fu, J. et al. Gold-catalyzed rearrangement of allylic oxonium ylides: efficient synthesis of highly functionalized dihydrofuran-3-ones. *Angew. Chem. Int. Ed.* **52**, 4198–4202 (2013).
26. Xiao, Y.-C. & Moberg, C. Silaborative carbocyclizations of 1,7-enynes. Diastereoselective preparation of chromane derivatives. *Org. Lett.* **18**, 308–311 (2016).

Acknowledgements

L.Z. thanks NIH (grant no. R01GM123342) and NSF CHE (grant no. 1800525) for financial support, and NSF (grant no. MRI-1920299) for the acquisition of Bruker 500 MHz and 400 MHz NMR instruments. The DFT studies were performed using the computational facilities purchased with funds from the National Science Foundation (grant no. CNS-1725797) and administered by the Center for Scientific Computing (CSC). The CSC is supported by the California NanoSystems Institute and the Materials Research Science and Engineering Center (MRSEC; NSF grant no. DMR 1720256) at UC Santa Barbara.

Author contributions

T.L. conducted the experiments and prepared a draft of the manuscript. X.C. synthesized the ligands and their gold catalysts and helped with the manuscript. P.Q. secured a postdoctoral fellowship from Wenzhou University for T.L. and participated in the chemistry design. L.Z. designed the chemistry and supervised its implementation and finalized the manuscript.

Competing interests

The authors declare no competing interests.

Additional information

Supplementary information The online version contains supplementary material available at https://doi.org/10.1038/s41929-020-00569-8.

Correspondence and requests for materials should be addressed to P.Q. or L.Z.

Peer review information Nature Catalysis thanks Ryan Vander Linden and the other, anonymous, reviewer(s) for their contribution to the peer review of this work.

Reprints and permissions information is available at www.nature.com/reprints.

Publisher's note Springer Nature remains neutral with regard to jurisdictional claims in published maps and institutional affiliations.